



OPEN RNF138 contributes to cisplatin resistance in nasopharyngeal carcinoma cells

Hangyu Xu^{1,4}, Qing Yin^{1,4}, Linna Fan², Yating Zhao³, Biying Song³, Qifan Xu³, Jie Zhu³✉ & Meifen Xu³✉

Resistance to chemotherapy is a significant concern in the treatment of nasopharyngeal carcinoma (NPC), and occurs due to various mechanisms. This study is aimed to evaluate the effects of RING finger protein 138 (RNF138) in the development of cisplatin resistance to NPC. After gene overexpression and silencing, the expression levels of RNF138 were evaluated. The impacts of RNF138 on the proliferation and apoptosis rate of NPC cells were then assessed. γ -H2AX-mediated DNA damage was determined via immunofluorescence assay. Moreover, a tumor xenograft mouse model was developed to investigate the role of RNF138 on NPC progression *in vivo*. Additionally, transcriptome analysis was performed in 5–8 F cells transfection with OE-RNF138 or OE-NC. Cisplatin significantly inhibited the proliferation, and promoted apoptosis and DNA damage in NPC cells; however, overexpression of RNF138 reversed the aforementioned regulatory role of cisplatin on NPC cells. Knockdown of RNF138 resulted in contrasting phenotypic outcomes. Additionally, in nude mice, RNF138 overexpression attenuated the suppressive effects of cisplatin on the growth of xenograft tumor, while RNF138 silencing further enhanced the inhibiting role of cisplatin. We further indicated that in 5–8 F cells following RNF138 overexpression, some pathways such as PI3K-Akt signaling pathway, human papillomavirus infection and ErbB signaling pathway that have been reported to be associated with NPC progression and cisplatin resistance were significantly enriched. These findings indicate that the modulation of RNF138 could potentially address the issue of chemotherapy failure by overcoming cisplatin resistance in NPC cells, making it a promising candidate for targeted drug therapy.

Keywords Nasopharyngeal carcinoma, RNF138, Cisplatin resistance, Proliferation, Apoptosis, DNA damage

Abbreviations

nasopharyngeal carcinoma	NPC
RING finger protein 138	RNF138
non-small cell lung cancer	NSCLC
lentiviral vector	LV
short hairpin RNA	sh-RNA
5-ethynyl-2'-deoxyuridine	EDU
differentially expressed genes	DEGs
Gene Ontology	GO
Kyoto Encyclopedia of Genes and Genomes	KEGG
4'	6-diamidino2-phenylindole, DAPI

Nasopharyngeal carcinoma (NPC) is a type of epithelial cancer that originates from the lining of the mucosa in the nasopharynx¹. The tumor is commonly found in the pharyngeal recess area. There are three different pathological subtypes of NPC, namely basaloid squamous, non-keratinising squamous and keratinising squamous. Among these subtypes, the non-keratinising subtype accounts for approximately 95% of cases in areas where NPC is prevalent². In fact, NPC has shown high sensitivity to both radiation therapy and chemotherapy. For patients with early stage or locally advanced NPC, treatment options often involve either radiotherapy alone

¹Department of Otolaryngology, Taizhou Central Hospital (Taizhou University Hospital), Taizhou 318000, Zhejiang, China. ²School of Laboratory Medicine and Life Sciences, Wenzhou Medical University, Wenzhou 325000, Zhejiang, China. ³Department of Clinical Laboratory, Taizhou Central Hospital (Taizhou University Hospital), No. 999 Donghai Avenue, Taizhou City 318000, Zhejiang Province, China. ⁴Hangyu Xu and Qing Yin contributed equally to this work. ✉email: zhuj9100@163.com; xumf9222@163.com

or a combination of chemotherapy and radiotherapy³. Although this combined approach has yielded satisfactory survival rates (approximately 90% for a period of five years)^{4,5}, there remains a subset of patients (8-10%) who experience recurrence and develop metastatic tumors^{6,7}. In cases where NPC recurs, multi-drug chemotherapy with cisplatin is considered as the standard treatment. However, overcoming chemoresistance poses significant challenges in effectively treating recurrent NPC patients⁸. Therefore, it holds immense importance to gain comprehensive understanding about the mechanisms underlying chemo-resistance in NPC.

E3 ubiquitin ligases serve as crucial elements in facilitating the ubiquitination process due to their precise regulation over both substrate affinity and specificity⁹. Over eight-hundred functional E3 ligases have been identified with potential roles¹⁰. The wide range of substrates associated with these ligases significantly contributes towards their multifaceted functionalities¹¹. Consequently, their involvement in regulating oncogenes and tumor suppressors establishes close links between E3 ligases and tumorigenesis¹². Moreover, considering the specific targeting capabilities exhibited by these enzymes towards substrates makes them promising candidates for developing anti-cancer drugs¹³. Notably, RING-box-containing E3 ligases known as RING finger proteins (RNFs) have emerged as significant contributors towards cisplatin resistance during cancer treatment. For instance, RNF38 has been suggested as a potential biomarker indicating a poor prognosis for non-small cell lung cancer (NSCLC), and when its expression is suppressed, NSCLC cells become more sensitive to cisplatin treatment¹⁴. It is worth noting that RNF138 belongs to the E3 ubiquitin ligase family and is initially identified in the Wnt signaling pathway¹⁵, comprising of a ubiquitin-interacting motif (UIM)-type domain, three zinc finger (ZNF) domains and a RING domain^{16,17}. RNF138 has been extensively studied for its involvement in human cancer development. For example, downregulation of RNF138 can impede the proliferative, migratory, and invasive capabilities of glioma cells¹⁸. Moreover, the ubiquitination activity mediated by RNF138 on ribosomal protein S3 (rpS3) protein is crucial for conferring resistance against radiation-induced apoptosis in glioblastoma cells¹⁹. Additionally, elevated expression levels of RNF138 have been observed in cisplatin-resistant gastric cancer (GC) cell lines compared to normal cell lines. Furthermore, manipulating the levels of RNF138 influences cisplatin resistance in these GC cells²⁰. Of utmost significance, a recent study conducted by Lei et al. screened a 6-gene signature including RNF138 to help the identification of individuals who would benefit from induction chemotherapy in patients with NPC²¹. Nevertheless, there remains limited knowledge regarding the involvement of RNF138 in the development of NPC and its potential role in conferring resistance to cisplatin.

In current study, we preliminarily hypothesized that RNF138 may regulate cisplatin resistance in NPC cells. The interactions between RNF138 expression and cisplatin for the proliferation, apoptosis and γ -H2AX-mediated DNA damage in NPC cells were explored. These results may provide a clinical therapeutic method for NPC patients with cisplatin resistance.

Methods

Cells and reagents

Human NPC cell lines (SUNE-2 and 5-8F) was obtained from Cell Bank of the Chinese Academy of Science (Shanghai, China). The cells underwent mycoplasma testing and were identified by STR without cross-contamination. DMEM, fetal bovine serum (FBS) and gentamicin were obtained from Gibco (Rockville, MD, USA). Cisplatin (purity $\geq 98\%$) was purchased from Solarbio LIFE SCIENCES Co., Ltd (Beijing, China). RNF138-siRNA1/2/3/4 and the negative control (si-NC) as well as overexpression of RNF138 (OE-RNF138) and the empty vector (OE-NC) were synthesized by VectorBuilder (Guangzhou, China). Lentiviral vectors (LV) for short hairpin RNA RNF138 (sh-RNF138), OE-RNF138 or LV-NC were constructed by Sangon Biotech (Shanghai, China). LIPOFECTAMINE 3000 and SUPERSCRIPT DOUBLE-STRANDE cDNA SYNTHESIS KIT were obtained from Invitrogen (Carlsbad, CA, USA). TOTAL RNA EXTRACTION KIT was acquired from Promega (Madison, WI, USA). The FIRST STRAND KIT and QUANTIFAST SYBR GREEN PCR KIT were obtained from Qiagen (Dusseldorf, GER). The ECL DETECTION KIT was obtained from Abbkine Scientific Co., Ltd (Wuhan, China). The BCA PROTEIN KIT was obtained from Biosharp Life Sciences (Hefei, China). RIPA LYSIS BUFFER was obtained from BOSTER Biological Technology Co., Ltd (Wuhan, China). Bovine serum albumin (BSA), primary antibodies (RNF138 and β -actin) and the corresponding HRP-conjugated secondary antibody were obtained from Thermo Fisher Scientific (Waltham, MA, USA). For Immunofluorescence tests, γ -H2AX primary antibody and IgG secondary antibody were acquired from Abcam (Cambridge, UK). The 5-ethynyl-2'-deoxyuridine (EDU) ASSAY KIT was procured from Ribo Biotechnology Co., Ltd (Guangzhou, China). The CCK-8 solution was purchased from Dojindo Laboratories (Shanghai, China). ANNEXIN V-FITC/PI APOPTOSIS DETECTION KIT was obtained from Vazyme (Nanjing, China).

Cell culture and transfection

SUNE-2 and 5-8 F cells were cultured in a CO₂ incubator at 37 °C with DMEM supplemented with 12 U/L gentamicin and 10% FBS. For transfection, LIPOFECTAMINE 3000 was used to deliver RNF138-siRNA1/2/3/4, si-NC, OE-RNF138 or OE-NC into SUNE-2 or 5-8 F cells (5×10^4) at room temperature for a duration of 48 h. The transfected cells were then harvested for subsequent experiments.

Total RNA isolation and qRT-PCR

Total RNA was extracted from 5 to 8 F and SUNE-2 cells using a TOTAL RNA EXTRACTION KIT, followed by cDNA synthesis with the assistance of the FIRST STRAND KIT. For qRT-PCR analysis, the QUANTIFAST SYBR GREEN PCR KIT was employed according to the provided instructions. The expression levels of RNF138 were determined using the $2^{-\Delta\Delta Ct}$ method, ensuring accurate normalization through the utilization of β -actin as an internal control. Please refer to Table 1 for a list of primers utilized in this study.

Gene	Sequences	
β -actin	Forward	5' - TGGACTTCGAGCAAGAGATG - 3'
	Reverse	5' - GAAGGAAGGCTGGAAGAGTG - 3'
RNF138	Forward	5' - CCACGTCTACACCGAAGAT - 3'
	Reverse	5' - GCATCTGCAGCTACCAGAAA - 3'

Table 1. Real-time PCR primer synthesis list.

Transcriptome analysis

Total RNA from 5 to 8 F cells transfection with OE-RNF1138 or OE-NC was isolated as described above. The RNA purification, reverse transcription, library construction, and sequencing were conducted by Majorbio Bio-pharm Biotechnology (Shanghai, China). Following the ILLUMINA directional protocol (Illumina, San Diego, CA USA), a total of 1 μ g RNA samples were utilized for the preparation of RNA-seq transcriptome libraries. In brief, messenger RNA was isolated using oligo (dT) beads through poly A selection method and subsequently fragmented using fragmentation buffer. Subsequently, double-stranded cDNA was synthesized utilizing a SUPERSCRIPT DOUBLE-STRANDE cDNA SYNTHESIS KIT with random hexamer primers from ILLUMINA. The synthesized cDNA underwent end-repair, phosphorylation and 'A' base addition as per ILLUMINA's library construction protocol. Libraries were size-selected for cDNA target fragments measuring 300 bp on 2% LOW RANGE ULTRA AGAROSE gel followed by PCR amplification employing PHUSION DNA POLYMERASE for 15 PCR cycles. After quantification using QUBIT 4.0 system, the paired-end RNA-seq sequencing library was sequenced utilizing the NOVASEQ 6000 sequencer.

The raw paired end reads underwent trimming and quality assessment using fastp²² with default settings. Subsequently, the resultant clean reads were individually aligned to a reference genome in orientation mode utilizing HISAT2 software²³. The assembled mapped reads for each sample were generated via STRINGTIE²⁴ using a reference-based methodology.

To identify differentially expressed genes (DEGs) among them, the expression level of each transcript was calculated according to the transcripts per million reads method. DEGs with $P < 0.05$ and $|\log_2(\text{Foldchange})| \geq 1$ were counted statistically significant. Gene Ontology (GO) and Kyoto Encyclopedia of Genes and Genomes (KEGG)^{25–27} (www.kegg.jp/kegg/kegg1.html) carried out by KOBAS²⁸ was used for enrichment analysis. The threshold used for KEGG pathway enrichment analysis is Corrected P-Value (qvalue) < 0.05 . Intelligent cluster analysis and visualization were performed by Visualization of filtered terms.

Western blotting

The 5–8 F cells were lysed using RIPA buffer, and protein concentration was determined utilizing a BCA PROTEIN KIT. Subsequently, the protein products underwent separation via SDS polyacrylamide gel electrophoresis and transfer onto PVDF membranes. To prevent nonspecific binding, we employed nonfat milk (5%) for membrane blocking. Following this step, the primary antibodies (RNF138 and β -actin; both diluted at 1:1000) were applied to the membranes for overnight incubation at 4 °C. Afterwards, the corresponding secondary antibody (diluted at 1:3000) was introduced and allowed to incubate for 1 h at room temperature. The immunoblotting results were visualized using an ECL DETECTION KIT.

CCK-8 assay

The viability of NPC cells was assessed using CCK-8 assays. 5–8 F or SUNE-2 cells (4×10^3 cells/well) were cultured in 96-well plates. After incubation for 48 and 72 h, the respective wells were added with 10 μ L of CCK-8 solution. The reaction was allowed to proceed for a duration of 3 h. The absorbance was measured at a wavelength of 450 nm using a BIOTEK microplate reader (Vermont, USA). The cell viability of each group was evaluated according to the absorbance value.

EDU proliferation assay

5–8 F or SUNE-2 cells were initially incubated with 50 μ M EDU at a temperature of 37 °C for a duration of 2 h. Subsequently, they were fixed using a solution containing 4% formaldehyde, and permeabilized by treating them with 0.5% TRITON X-100 for a period of 20 min. Following this, the cells were incubated with an APOLLO REACTION COCKTAIL (1 \times) at room temperature for approximately half an hour. To visualize DNA, DAPI (4',6-diamidino2-phenylindole) was employed as a staining agent for an additional duration of 30 min. A fluorescence microscope (Carl Zeiss, Oberkochen, Germany) was utilized to observe the EDU-positive cells (scale bar = 100 μ m).

Flow cytometry analysis

The apoptosis rate of NPC cells was evaluated by employing an ANNEXIN V-FITC/PI APOPTOSIS DETECTION KIT as per the instructions provided by the manufacturer. A total of 2×10^5 re-suspended 5–8 F or SUNE-2 cells were subjected to staining with Annexin V-FITC (10 μ L) and PI (5 μ L) at a temperature of 25 °C for a duration of 15 min in darkness, followed by the addition of binding buffer (500 μ L). Subsequently, flow cytometry analysis using a FACSCAN INSTRUMENT (BD Biosciences, Franklin Lakes, NJ, USA) was performed to assess apoptotic cell population.

DNA damage immunofluorescence analysis

The re-suspended 5–8 F or SUNE-2 cells were cultured in 96-well plates and fixed using a solution of 4% buffered paraformaldehyde. Permeabilization was achieved by treating the cells with 1% TRITON X-100 once cell fusion reached at 80–90%. Following a blocking step with a solution of 1% BSA for 30 min, the cells were incubated with an antibody specific to γ -H2AX (diluted at 1:250) at a temperature of 37 °C for a duration of 2 h. Subsequently, the cells were exposed to a secondary IgG antibody (diluted at 1:5000) for one hour at the same temperature. Finally, DAPI staining was performed by incubating the cells at 37 °C for 5 min. The resulting images were captured and analyzed using a fluorescence microscopy (scale bar = 25 μ m).

Tumor xenografts in nude mice

Four-week-old BALB/c-nu nude mice were obtained from Huafukang (Beijing, China) and tamed for at least 1 week. The mice were randomly divided into 4 groups: model, LV-NC + cisplatin, sh-RNF138 + cisplatin and OE-RNF138 + cisplatin, with each group comprising six mice. SUNE2 cells (2×10^6 cells) transfected with LV-NC, sh-RNF138 or OE-RNF138 were subcutaneously injected into the right flank of mice. One week later, cisplatin was administered by intraperitoneal injection at a dose of 5 mg/kg, once every three days. Tumor volume was measured at 7th, 14th, 21st and 28th day, using the formula: $V = \text{length} \times \text{width}^2 \times 0.5$. Four weeks later, mice were euthanatized via an overdose of sodium pentobarbital (200 mg/kg) and the tumor xenografts were excised. The experiments in this study were conducted by two experienced technicians who were unaware of the group assignments. The study is reported in accordance with ARRIVE guidelines (<https://arriveguidelines.org>). Animal experiments were performed in accordance with the NIH Guide for the Care and Use of Laboratory Animals and approved by the Ethics Committee of Taizhou Central Hospital (Taizhou University Hospital) (approval number: 2019-54).

Immunohistochemistry

The xenografts underwent fixation, paraffin embedding, dewaxing, and rehydration. Following antigen retrieval, the samples were subjected to overnight incubation at 4 °C with primary antibody RNF138 (1:500), followed by a 1-hour incubation at 37 °C with HRP-conjugated secondary antibody (1:3000). Subsequently, each slice was stained using DAB and images were captured under a light microscope (scale bar = 100 μ m).

Statistical analysis

Data analysis was performed using SPSS software version 20.0 (SPSS Inc., Chicago, IL, USA) and presented as the mean \pm standard deviation (SD). Differences between two groups or among multiple groups were determined using Student's t-test or one-way ANOVA followed by Tukey's post-hoc test. $P < 0.05$ was counted as statistically significant.

Results

RNF138 expression after transfection

The expression of RNF138 after transfection was determined. As illustrated in Fig. 1A, the mRNA expression and protein level of RNF138 was significantly increased following OE-RNF138 transfection ($P < 0.001$). Additionally, siRNA1/2/3/4 was introduced into 5–8 F cells to measure RNF138 expression levels. It was shown that transfection of siRNA1 and siRNA2 decreased the mRNA expression and protein level of RNF138 remarkably (Fig. 1B, $P < 0.001$). Therefore, both siRNA1 and siRNA2 were selected for subsequent experiments.

Effects of RNF138 on the proliferation of cisplatin-treated NPC cells

After OE-RNF138 transfection, the cell viability of 5–8 F and SUNE-2 cells at 48 and 72 h was ascertained. We found that at 48 and 72 h, the cell viability could be inhibited by cisplatin treatment, but promoted after OE-RNF138 transfection (Fig. 2A, $P < 0.05$). Meanwhile, the results further demonstrated that overexpression of RNF138 attenuated the inhibiting effects of cisplatin treatment on cell viability ($P < 0.01$). On the contrary, transfection of siRNA1 or siRNA2 further enhanced the inhibiting capacities of cisplatin treatment on cell viability at 48 and 72 h (Fig. 2B, $P < 0.05$). To delve deeper into the cellular growth mechanism, we conducted EDU assays to investigate how RNF138 influences the regulation of DNA replication. Compared to the OE-NC group, EDU-staining cells were remarkably decreased in OE-NC + cisplatin group (Fig. 2C, $P < 0.001$), but were increased in the OE-RNF138 group ($P < 0.05$). Compared with the OE-NC + cisplatin group, the percentage of EDU-staining cells was restored to some extent ($P < 0.05$). The opposite patterns were observed in the results of siRNA transfection (Fig. 2D, $P < 0.05$).

Effects of RNF138 on the apoptosis of cisplatin-treated NPC cells

Flow cytometer was used to assess the apoptosis rate of NPC cells following transfection. As illustrated in Fig. 3A, by contrast to the OE-NC group, the apoptosis rate of 5–8 F and SUNE-2 cells was markedly increased in the OE-NC + cisplatin group ($P < 0.01$), while was inhibited in the OE-RNF138 group ($P < 0.001$). Compared to the OE-NC + cisplatin group, the apoptosis rate in the OE-RNF138 + cisplatin group was significantly decreased ($P < 0.01$). Following transfection of siRNA1 and siRNA2, the apoptosis rate of 5–8 F and SUNE-2 cells was distinctly accelerated (Fig. 3B, $P < 0.001$). Additionally, we demonstrated that silencing of RNF138 further enhanced the promoting effects of cisplatin on the apoptosis rate of 5–8 F and SUNE-2 cells (Fig. 3B, $P < 0.001$).

Overexpression of RNF138 attenuates DNA damage in NPC cells induced by cisplatin

To investigate the effects of RNF138 overexpression on DNA damage of cisplatin-treated NPC cells, the fluorescence intensity of γ -H2AX (a DNA damage marker) was determined via immunofluorescence assay. As depicted in Fig. 4A-B, the fluorescence intensity of γ -H2AX in cisplatin-treated NPC cells (5–8 F and SUNE-2) was

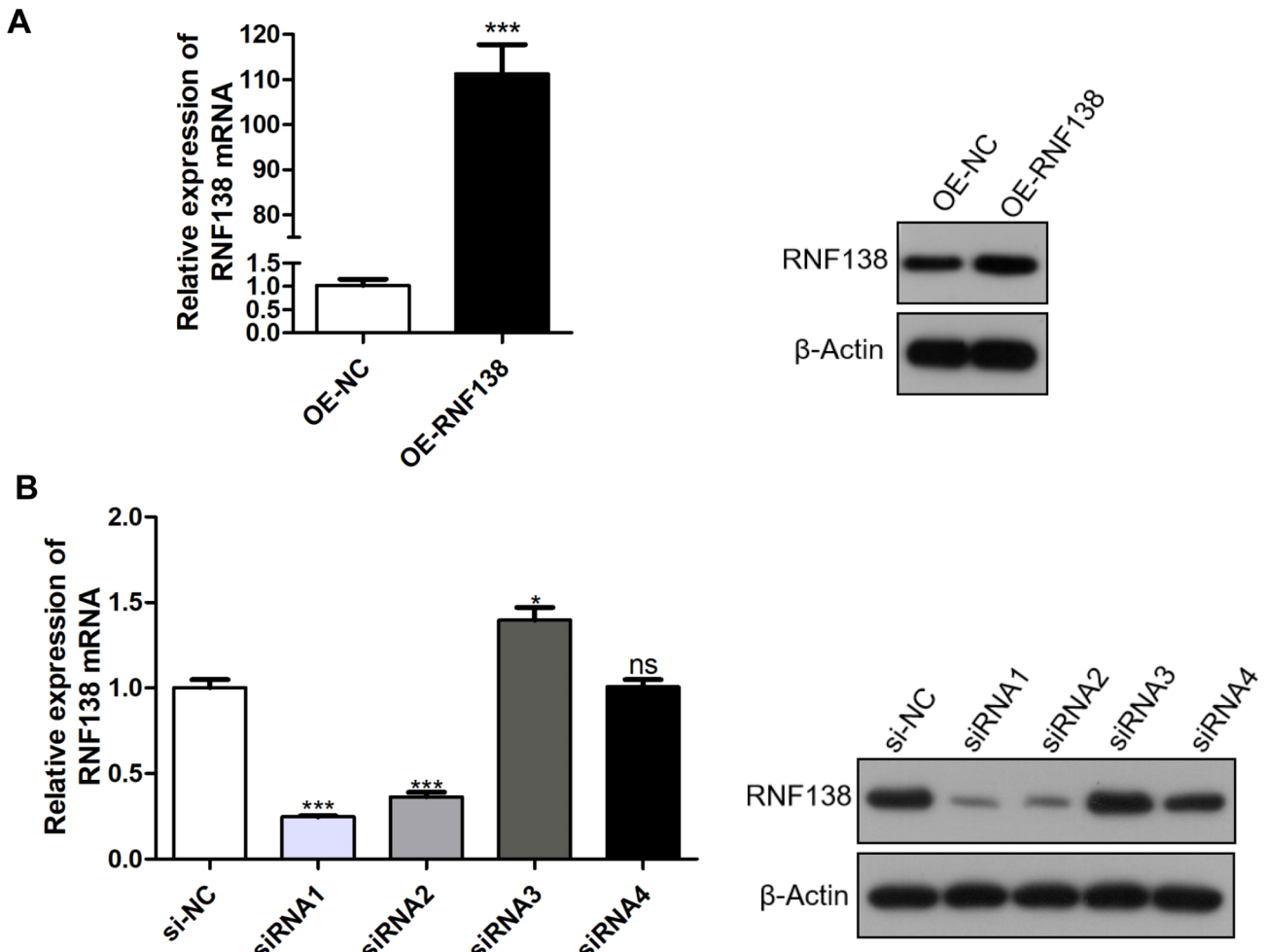


Fig. 1. RNF138 expression after transfection. (A) The mRNA expression and protein level of RNF138 in 5–8 F cells transfected with OE-NC or OE-RNF138 were determined by qRT-PCR and western blotting, respectively. *** $P < 0.001$ vs. OE-NC. (B) The mRNA expression and protein level of RNF138 in 5–8 F cells transfected with si-NC or siRNA1/2/3/4 were determined by qRT-PCR and western blotting, respectively. * $P < 0.05$, *** $P < 0.001$ vs. si-NC. ns: no significance.

significantly enhanced, while transfection of OE-RNF138 had almost no influence upon γ -H2AX fluorescence intensity. However, it can be clearly observed that the fluorescence intensity of γ -H2AX was attenuated to some extent compared to the OE-NC + cisplatin group. These results indicating that RNF138 overexpression could protect against DNA damage caused by cisplatin.

Effects of RNF138 on the growth of xenograft tumor in a mouse model

The representative images of xenograft mice were shown in Fig. 5A. The tumor volume was measured every week and xenograft tumors in different groups were collected at the end of 28 days. As illustrated in Fig. 5B, we found that tumor volume in the LV-NC + cisplatin group was dramatically reduced compared to that of model group ($P < 0.001$). However, compared with the LV-NC + cisplatin group, tumor volume was larger in the OE-RNF138 + cisplatin group ($P < 0.01$), while was further lower in the sh-RNF138 + cisplatin group ($P < 0.05$). The results of immunohistochemistry showed that RNF138 expression was significantly decreased in the sh-RNF138 + cisplatin group, but was increased in OE-RNF138 + cisplatin group.

Transcriptomics expression profile analysis of 5–8 F cells transfection of OE-RNF138

Transcriptome differential expression analysis revealed that a total of 8348 DEGs in 5–8 F cells following transfection of OE-RNF138, among which 4643 genes were upregulated and 3705 genes were downregulated in the OE-RNF138 group (Fig. 6A). GO and KEGG enrichment analyses indicated that cell adhesion, angiogenesis, pathways in cancer and transcriptional mis-regulation in cancer were significantly enriched in the OE-RNF138 group (Fig. 6B). Additionally, we further demonstrated that cluster 1 and cluster 6 were mainly associated with PI3K-Akt signaling pathway, human papillomavirus infection and ErbB signaling pathway (Fig. 6C). More importantly, these pathways have been reported to be associated with NPC progression and cisplatin resistance^{29–32}. These results further validated our preliminary hypothesis.

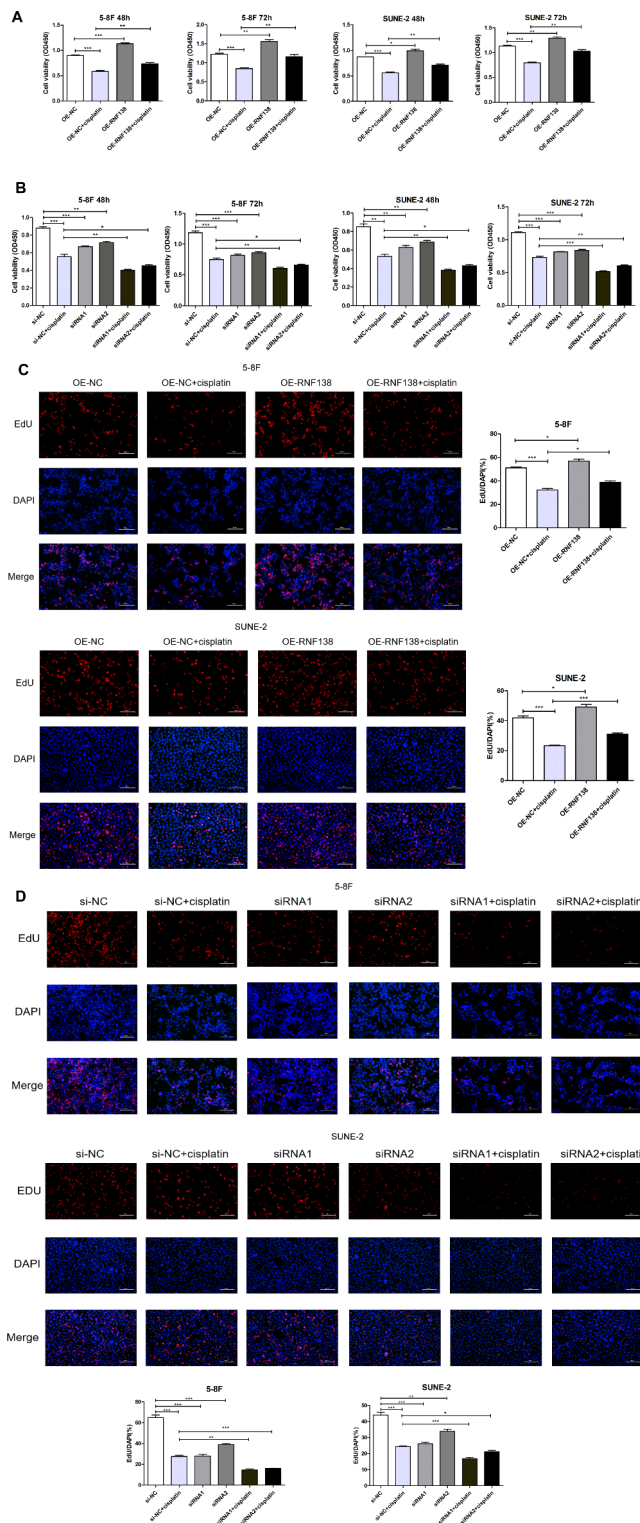


Fig. 2. Effects of RNF138 on the proliferation of cisplatin-treated NPC cells. (A) The viability of cisplatin-treated 5-8 F and SUNE-2 cells that were transfected with OE-NC or OE-RNF138 was measured by CCK-8 assays at 48 and 72 h. (B) The viability of cisplatin-treated 5-8 F and SUNE-2 cells that were transfected with si-NC or siRNA1/2 was measured by CCK-8 assays at 48 and 72 h. (C) DNA replication in cisplatin-treated 5-8 F and SUNE-2 cells that were transfected with OE-NC or OE-RNF138 was determined by the EDU assay. (D) DNA replication in cisplatin-treated 5-8 F and SUNE-2 cells that were transfected with si-NC or siRNA1/2 was determined by the EDU assay. * $P < 0.05$, ** $P < 0.01$, *** $P < 0.001$. scale bar = 100 μ m.

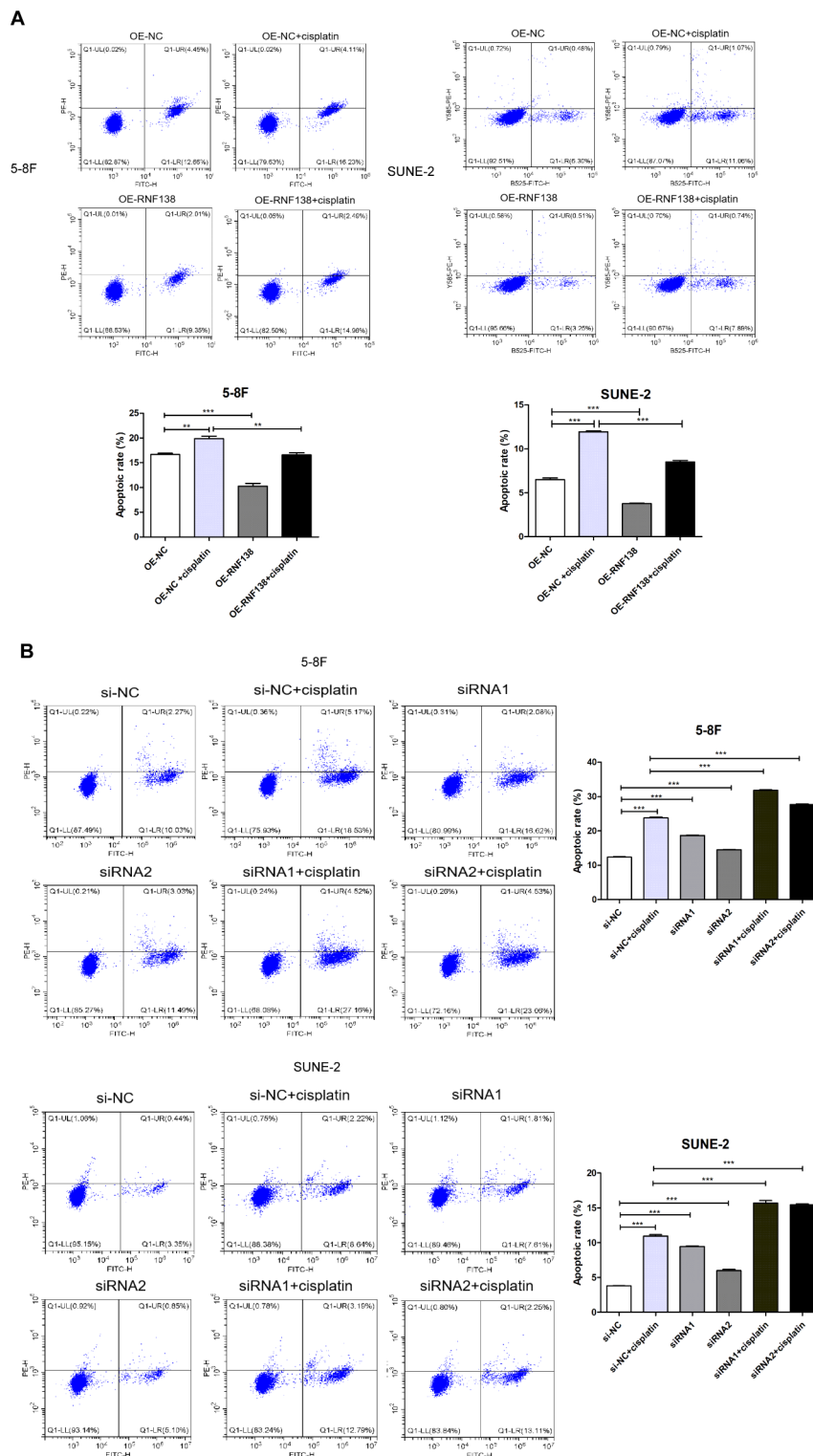


Fig. 3. Effects of RNF138 on the apoptosis of cisplatin-treated NPC cells. (A) The apoptosis rate of cisplatin-treated 5-8 F and SUNE-2 cells that were transfected with OE-NC or OE-RNF138 was assessed by flow cytometry analysis. (B) The apoptosis rate of cisplatin-treated 5-8 F and SUNE-2 cells that were transfected with si-NC or siRNA1/2 was assessed by flow cytometry analysis. ** $P < 0.01$, *** $P < 0.001$.

Discussion

The incidence of NPC is infrequent in the majority of countries globally, typically exhibiting age-standardized rates lower than 1 per 100,000 population³³. According to data from the International Agency for Research on Cancer, NPC accounted for only 0.7% of all cancer cases diagnosed in 2020, with approximately 130,000 new

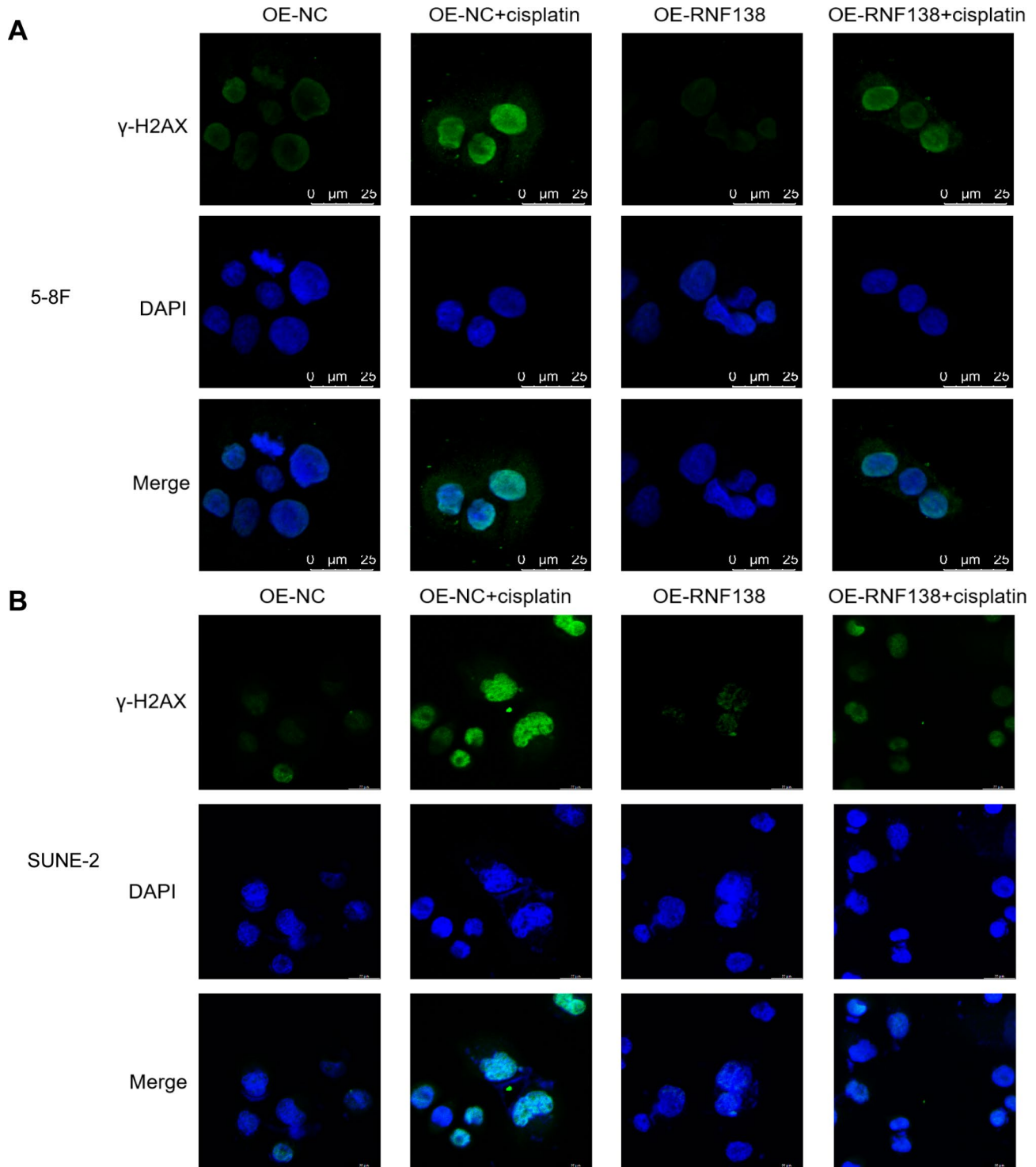


Fig. 4. Overexpression of RNF138 attenuates DNA damage in NPC cells induced by cisplatin. (A-B) Immunofluorescence staining was performed to verify the positive expression of γ -H2AX in cisplatin-treated 5-8 F and SUNE-2 cells that were transfected with OE-NC or OE-RNF138. scale bar = 25 μ m.

cases reported³⁴. The majority of these cases (over 70%) were found in East and Southeast Asia, particularly in South China which has a high incidence rate³⁴. In China, the age-standardized mortality rate for NPC is about twice as high as the global average at 1.6 per 100,000 population³⁴. The standard approach for treating locally advanced nasopharyngeal carcinoma involves combining cisplatin-based chemotherapy with radiotherapy. Despite showing promising results, many patients continue to suffer from significant side effects during their treatment course³⁵. Consequently, enhancing the effectiveness of chemotherapy remains a major challenge in managing this particular form of cancer.

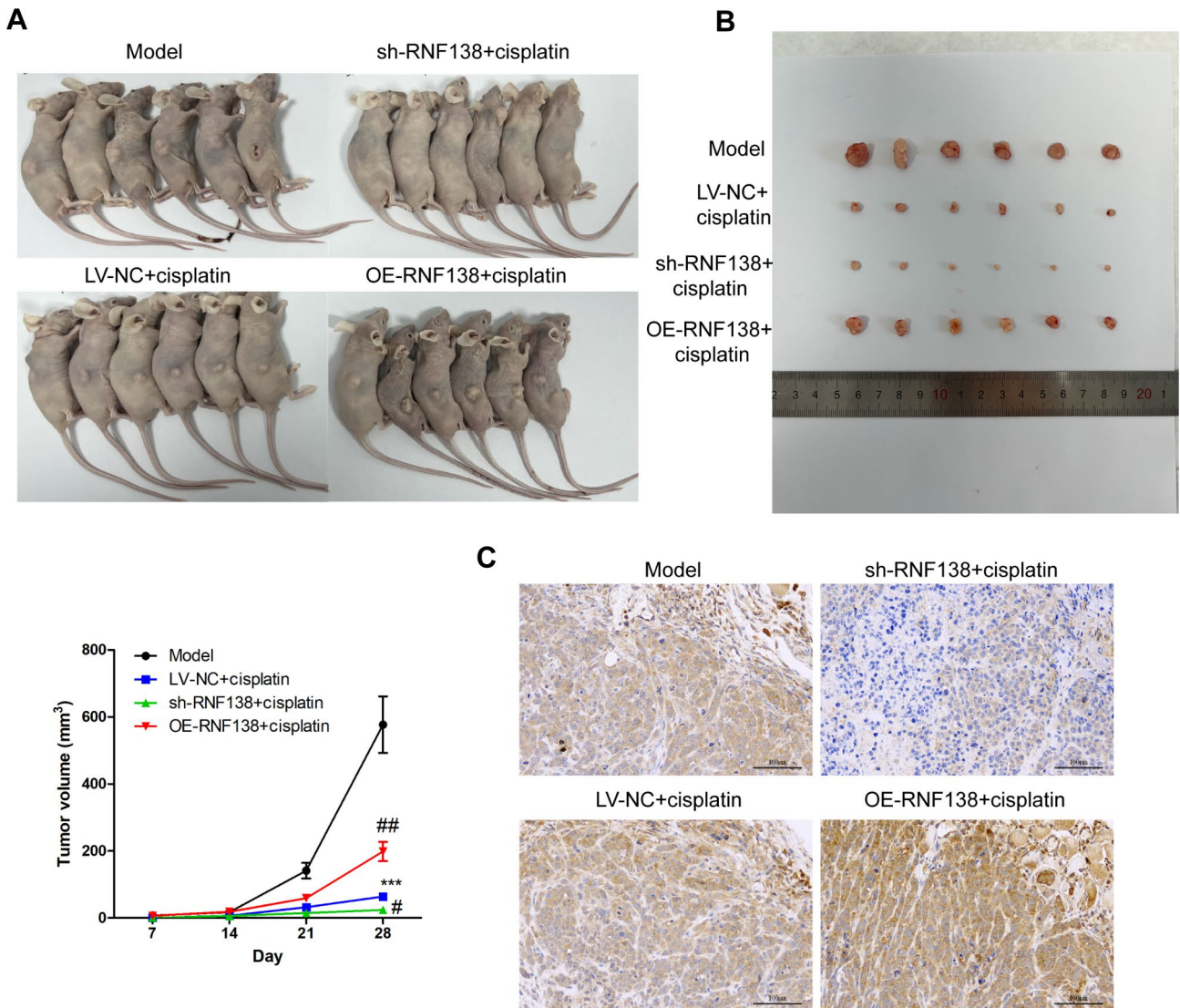


Fig. 5. Effects of RNF138 on the growth of xenograft tumor in a mouse model. (A) The representative images of xenograft tumors. (B) Tumor volume was measured at 7th, 14th, 21st and 28th day. (C) The expression levels of RNF138 in xenograft tumors of different groups were assessed through immunohistochemistry. *** $P < 0.001$ vs. model. # $P < 0.05$, ## $P < 0.01$ vs. LV-NC + cisplatin. scale bar = 100 μ m.

Resistance to chemotherapy is a significant concern in the treatment of NPC, and occurs due to various mechanisms. In 2021, Lei et al. reported six gene-expression predictors to assess the efficacy of induction chemotherapy in patients with locoregionally advanced NPC, among which includes AL161418.1, LRRD1, OGFRL1, PLAC8, PTGS2 and RNF138²¹. In our pre-experiments, the expression of these six genes in tumor tissues of NPC patients was preliminarily determined. The results showed that RNF138 exhibited the highest level of expression among the six genes in tumor tissues (data were not shown), indicating that RNF138 may be an oncogene in NPC tumorigenesis. Meanwhile, we performed transcriptome analysis in 5–8 F cells that were transfected with OE-RNF138. We found that in OE-RNF139 samples, the enrichment pathways such as PI3K-Akt signaling pathway, human papillomavirus infection and ErbB signaling pathway were strong associated with NPC progression and cisplatin resistance as previously described^{29–32}. Therefore, we selected RNF138 to explore its potential role in conferring resistance to cisplatin in the development of NPC. All tumors possess the capability to undergo uncontrolled growth, surpassing the limitations observed in normal tissue. Deviations in the regulation of a limited number of crucial pathways governing cell proliferation and survival are essential for the development of all tumors. Therefore, unregulated cell proliferation, coupled with inhibited apoptosis, form the fundamental basis upon which neoplastic progression takes place³⁶. In our study, as expected, we found that cisplatin exerts an important inhibiting role in NPC progression in vitro, namely inhibiting NPC cell proliferation and promoting apoptosis. Meanwhile, we further demonstrated the overexpressed RNF138 attenuated the regulating effects of cisplatin on NPC cells, while knockdown of RNF138 enhanced the inhibiting role of cisplatin in cell proliferation and the promoting role in apoptosis. Similarly, a recent study written by Lu et al. has uncovered that RNF138 upregulation enhances the survival of GC cells and reduces apoptosis

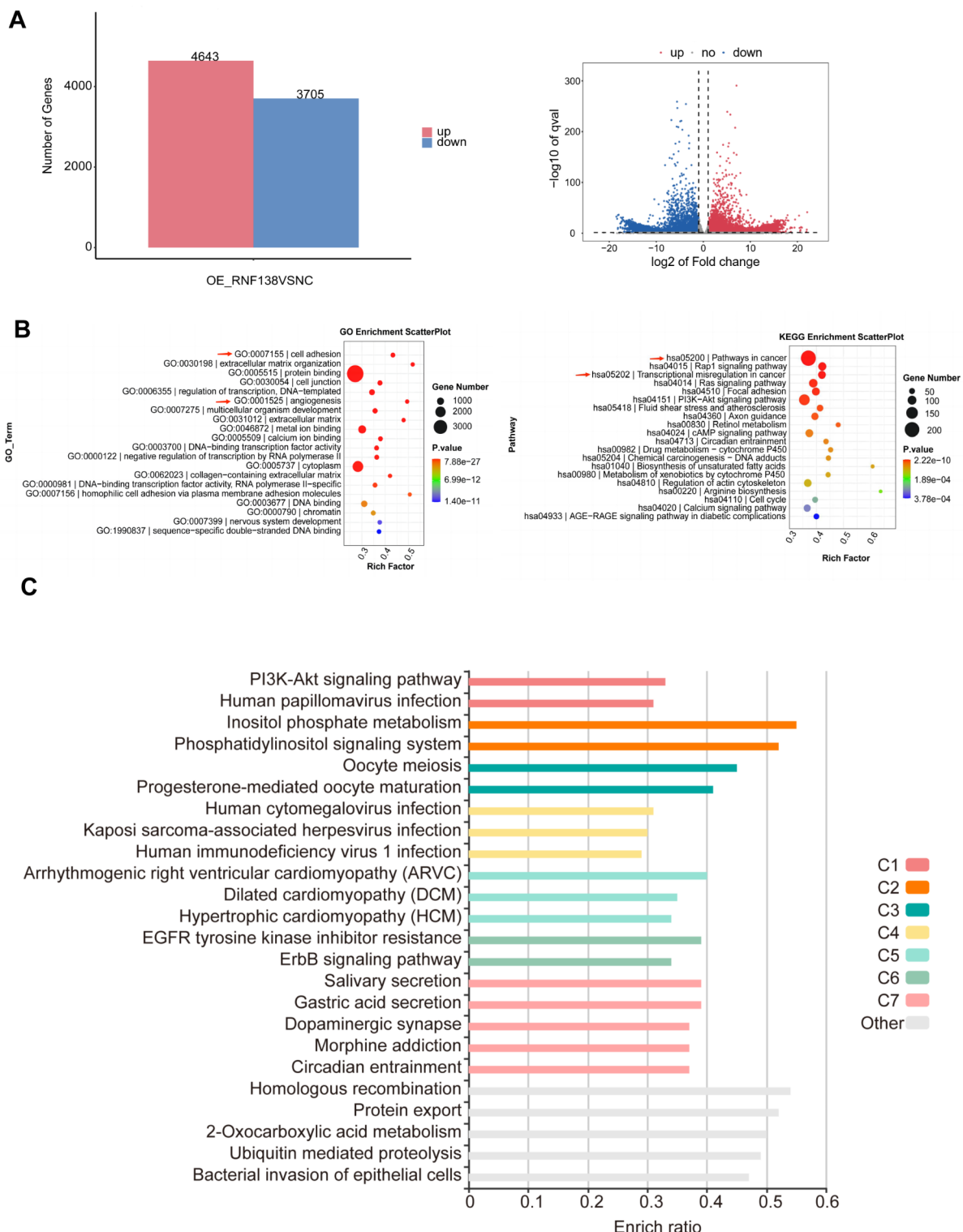


Fig. 6. Transcriptomics expression profile analysis of 5–8 F cells transfected with OE-RNF138. (A) The column diagram and volcano plot of differentially expressed genes (DEGs) between OE-NC and OE-RNF138. (B) Gene Ontology (GO) and Kyoto Encyclopedia of Genes and Genomes (KEGG) (www.kegg.jp/kegg/kegg1.html) was used for enrichment analysis of the DEGs between OE-NC and OE-RNF138. (C) Cluster analysis between OE-NC and OE-RNF138.

in cisplatin-sensitive GC cells, whereas RNF138 downregulation leads to contrasting outcomes in cisplatin-resistant cells, indicating that RNF138 confers cisplatin resistance in GC cells²⁰. These results implied that RNF138 may also induce cisplatin resistance in NPC cells. Additionally, we further demonstrated that in nude mice, RNF138 overexpression attenuated the suppressive effects of cisplatin on the growth of xenograft tumor, while RNF138 silencing further enhanced the inhibiting role of cisplatin. Collectively, we believed that RNF138 confers cisplatin resistance in NPC cells through promoting proliferation and inhibiting apoptosis.

Another key finding of our study is that RNF overexpression can attenuate cisplatin-induced DNA damage in NPC cells. It is widely recognized that cisplatin possesses potent DNA-damaging properties, leading to the activation of crucial transcription factors in response to DNA repair³⁷. The immunofluorescence results revealed a notable increase in the fluorescence intensity of γ -H2AX in NPC cells treated with cisplatin, whereas it exhibited a substantial reduction after transfection with OE-RNF138. These results suggested that RNF138 plays a crucial role in the repair of DNA damage caused by cisplatin-induced stress. Of course, previous study has reported that cisplatin has the ability to create crosslinks within and between purines in DNA³⁸. It is probable that these adducts formed by cisplatin and DNA cannot be utilized for gene transcription, as they are essential for the unwinding and opening of double strands of DNA³⁸. Therefore, future research is necessary to further analyze the mechanisms that underlie the specific function of RNF138 in repairing DNA damage in DNA repair of cisplatin-resistant NPC.

There is a limitation of this study that should not be neglected. For in vitro experiments, adding the bar graphs for parental cell lines without any transfection is more rigorous for this study. We will consider this in future studies.

Conclusions

In summary, the current study uncovers the potential role of RNF138 in conferring resistance to cisplatin in NPC, indicating that RNF138 can enhance cisplatin resistance in NPC cells by promoting proliferation, inhibiting apoptosis and attenuating γ -H2AX-mediated DNA damage. This may contribute information and insights on possible clinical therapeutic therapies for NPC patients with cisplatin resistance.

Data availability

The data analyzed during the current study are available from the corresponding author on reasonable request.

Received: 10 September 2024; Accepted: 6 January 2025

Published online: 09 January 2025

References

1. Jicman Stan, D. et al. Nasopharyngeal carcinoma: a new synthesis of literature data (review). *Exp. Ther. Med.* **23**, 136. <https://doi.org/10.3892/etm.2021.11059> (2022).
2. Cantu, G. Nasopharyngeal carcinoma. A different head and neck tumour. Part A: from histology to staging. *Acta Otorhinolaryngol. Ital.* **43**, 85–98. <https://doi.org/10.14639/0392-100X-N2222> (2023).
3. Caudell, J. J. et al. NCCN Guidelines(R) insights: Head and Neck cancers, Version 1.2022. *J. Natl. Compr. Canc Netw.* **20**, 224–234. <https://doi.org/10.6004/jnccn.2022.0016> (2022).
4. Jiromaru, R., Nakagawa, T. & Yasumatsu, R. Advanced Nasopharyngeal Carcinoma: current and emerging treatment options. *Cancer Manag. Res.* **14**, 2681–2689. <https://doi.org/10.2147/CMAR.S341472> (2022).
5. Jen, C. W. et al. Evaluating the efficacy of different treatment intensities in nasopharyngeal carcinoma patients: a Nationwide Cancer Registry-based study. *Ann. Surg. Oncol.* <https://doi.org/10.1245/s10434-024-16145-4> (2024).
6. Peng, Z. et al. Treatment of recurrent nasopharyngeal carcinoma: a sequential challenge. *Cancers (Basel)* **14**. <https://doi.org/10.3390/cancers14174111> (2022).
7. Juarez-Vignon Whaley, J. J. et al. Recurrent/Metastatic nasopharyngeal carcinoma treatment from Present to Future: where are we and where are we heading? *Curr. Treat. Options Oncol.* **24**, 1138–1166. <https://doi.org/10.1007/s11864-023-01101-3> (2023).
8. Perri, F. et al. Management of recurrent nasopharyngeal carcinoma: current perspectives. *Oncotargets Ther.* **12**, 1583–1591. <https://doi.org/10.2147/OTT.S188148> (2019).
9. Yang, Q., Zhao, J., Chen, D. & Wang, Y. E3 ubiquitin ligases: styles, structures and functions. *Mol. Biomed.* **2**, 23. <https://doi.org/10.1186/s43556-021-00043-2> (2021).
10. Liu, Y., Duan, C. & Zhang, C. E3 ubiquitin ligase in Anticancer Druggs Resistance: recent advances and future potential. *Front. Pharmacol.* **12**, 645864. <https://doi.org/10.3389/fphar.2021.645864> (2021).
11. Sampson, C. et al. The roles of E3 ubiquitin ligases in cancer progression and targeted therapy. *Clin. Transl Med.* **13**, e1204. <https://doi.org/10.1002/ctm2.1204> (2023).
12. Saravanan, K. M., Kannan, M., Meera, P., Bharathkumar, N. & Anand, T. E3 ligases: a potential multi-drug target for different types of cancers and neurological disorders. *Future Med. Chem.* **14**, 187–201. <https://doi.org/10.4155/fmc-2021-0157> (2022).
13. Ye, P. et al. Potential of E3 Ubiquitin Ligases in Cancer Immunity: Opportunities and Challenges. *Cells* **10**, (2021). <https://doi.org/10.3390/cells10123309>
14. Wu, C., Chen, L., Tao, H., Kong, L. & Hu, Y. RING finger protein 38 induces the drug resistance of cisplatin in non-small-cell lung cancer. *Cell. Biol. Int.* **45**, 287–294. <https://doi.org/10.1002/cbin.11423> (2021).
15. Cruz, L., Soares, P. & Correia, M. Ubiquitin-specific proteases: players in Cancer Cellular processes. *Pharmaceuticals (Basel)* **14**. <https://doi.org/10.3390/ph14090848> (2021).
16. Cai, C., Tang, Y. D., Zhai, J. & Zheng, C. The RING finger protein family in health and disease. *Signal. Transduct. Target. Ther.* **7**, 300. <https://doi.org/10.1038/s41392-022-01152-2> (2022).
17. Zeng, X. et al. RNF138 downregulates antiviral innate immunity by inhibiting IRF3 activation. *Int. J. Mol. Sci.* **24** <https://doi.org/10.3390/ijms242216110> (2023).
18. Wu, H. et al. [Corrigendum] downregulation of RNF138 inhibits cellular proliferation, migration, invasion and EMT in glioma cells via suppression of the Erk signaling pathway. *Oncol. Rep.* **48** <https://doi.org/10.3892/or.2022.8337> (2022).
19. Kim, W. et al. RNF138-mediated ubiquitination of rpS3 is required for resistance of glioblastoma cells to radiation-induced apoptosis. *Exp. Mol. Med.* **50**, e434. <https://doi.org/10.1038/emm.2017.247> (2018).
20. Lu, Y. et al. RNF138 confers cisplatin resistance in gastric cancer cells via activating Chk1 signaling pathway. *Cancer Biol. Ther.* **19**, 1128–1138. <https://doi.org/10.1080/15384047.2018.1480293> (2018).

21. Lei, Y. et al. A gene-expression predictor for efficacy of induction chemotherapy in Locoregionally Advanced Nasopharyngeal Carcinoma. *J. Natl. Cancer Inst.* **113**, 471–480. <https://doi.org/10.1093/jnci/djaa100> (2021).
22. Chen, S. Ultrafast one-pass FASTQ data preprocessing, quality control, and deduplication using fastp. *Imeta* **2**, e107. <https://doi.org/10.1002/im2.107> (2023).
23. Kim, D., Langmead, B. & Salzberg, S. L. HISAT: a fast spliced aligner with low memory requirements. *Nat. Methods* **12**, 357–360. <https://doi.org/10.1038/nmeth.3317> (2015).
24. Shumate, A., Wong, B., Pertea, G. & Pertea, M. Improved transcriptome assembly using a hybrid of long and short reads with StringTie. *PLoS Comput. Biol.* **18**, e1009730. <https://doi.org/10.1371/journal.pcbi.1009730> (2022).
25. Kanehisa, M. & Goto, S. KEGG: kyoto encyclopedia of genes and genomes. *Nucleic Acids Res.* **28**, 27–30. <https://doi.org/10.1093/nar/28.1.27> (2000).
26. Kanehisa, M. Toward understanding the origin and evolution of cellular organisms. *Protein Sci.* **28**, 1947–1951. <https://doi.org/10.1002/pro.3715> (2019).
27. Kanehisa, M., Furumichi, M., Sato, Y., Kawashima, M. & Ishiguro-Watanabe, M. KEGG for taxonomy-based analysis of pathways and genomes. *Nucleic Acids Res.* **51**, D587–D592. <https://doi.org/10.1093/nar/gkac963> (2023).
28. Bu, D. et al. KOBAS-i: intelligent prioritization and exploratory visualization of biological functions for gene enrichment analysis. *Nucleic Acids Res.* **49**, W317–W325. <https://doi.org/10.1093/nar/gkab447> (2021).
29. Hung, S. H., Yang, T. H., Cheng, Y. F., Chen, C. S. & Lin, H. C. Association of Nasopharynx Cancer with Human Papillomavirus infections. *Cancers (Basel)*, **15**. <https://doi.org/10.3390/cancers15164082> (2023).
30. Zhang, P. et al. Mir-205-5p regulates epithelial-mesenchymal transition by targeting PTEN via PI3K/AKT signaling pathway in cisplatin-resistant nasopharyngeal carcinoma cells. *Gene* **710**, 103–113. <https://doi.org/10.1016/j.gene.2019.05.058> (2019).
31. Navaei, Z. N., Khalili-Tanha, G., Zangouei, A. S., Abbaszadegan, M. R. & Moghboli, M. PI3K/AKT signaling pathway as a critical regulator of cisplatin response in tumor cells. *Oncol. Res.* **29**, 235–250. <https://doi.org/10.32604/or.2022.025323> (2021).
32. Peng, L. X. et al. LACTB promotes metastasis of nasopharyngeal carcinoma via activation of ERBB3/EGFR-ERK signaling resulting in unfavorable patient survival. *Cancer Lett.* **498**, 165–177. <https://doi.org/10.1016/j.canlet.2020.10.051> (2021).
33. Chang, E. T., Ye, W., Zeng, Y. X. & Adami, H. O. The evolving epidemiology of nasopharyngeal carcinoma. *Cancer Epidemiol. Biomarkers Prev.* **30**, 1035–1047. <https://doi.org/10.1158/1055-9965.EPI-20-1702> (2021).
34. Sung, H. et al. Global Cancer statistics 2020: GLOBOCAN estimates of incidence and Mortality Worldwide for 36 cancers in 185 countries. *CA Cancer J. Clin.* **71**, 209–249. <https://doi.org/10.3322/caac.21660> (2021).
35. Liu, Z., Chen, Y., Su, Y., Hu, X. & Peng, X. Nasopharyngeal carcinoma: clinical achievements and considerations among Treatment options. *Front. Oncol.* **11**, 635737. <https://doi.org/10.3389/fonc.2021.635737> (2021).
36. Liu, J. et al. Deubiquitinases in cancers: aspects of Proliferation, Metastasis, and apoptosis. *Cancers (Basel)*, **14**. <https://doi.org/10.390/cancers14143547> (2022).
37. de Almeida, L. C., Calil, F. A. & Machado-Neto, J. A. Costa-Lotufo, L. V. DNA damaging agents and DNA repair: from carcinogenesis to cancer therapy. *Cancer Genet.* **252–253**, 6–24. <https://doi.org/10.1016/j.cancergen.2020.12.002> (2021).
38. Slyskova, J. et al. Detection of oxaliplatin- and cisplatin-DNA lesions requires different global genome repair mechanisms that affect their clinical efficacy. *NAR Cancer*, **5**, zcad057. <https://doi.org/10.1093/narcan/zcad057> (2023).

Acknowledgements

Not applicable.

Author contributions

Jie Zhu and Meifen Xu made substantial contributions to the conception and design of the study. All authors made substantial contributions to data acquisition, quality control of data and algorithms, data analysis and interpretation, and statistical analysis. Hangyu Xu and Qing Yin made substantial contributions to manuscript preparation and editing. All authors made substantial contributions to manuscript review. All authors have read and approved the final manuscript.

Funding statement

This study was funded by Taizhou Municipal Bureau of Science and Technology (No. 1901ky43).

Declarations

Consent for publication

Not applicable.

Competing interests

The authors declare no competing interests.

Conflict of interest

The authors declare no conflicts of interest.

Ethics approval statement

This study was approved by the Ethical Committee of Taizhou Central Hospital (Taizhou University Hospital) (approval number: 2019-54).

Permission to reproduce material from other sources

Not applicable.

Additional information

Supplementary Information The online version contains supplementary material available at <https://doi.org/10.1038/s41598-025-85716-6>.

Correspondence and requests for materials should be addressed to J.Z. or M.X.

Reprints and permissions information is available at www.nature.com/reprints.

Publisher's note Springer Nature remains neutral with regard to jurisdictional claims in published maps and institutional affiliations.

Open Access This article is licensed under a Creative Commons Attribution-NonCommercial-NoDerivatives 4.0 International License, which permits any non-commercial use, sharing, distribution and reproduction in any medium or format, as long as you give appropriate credit to the original author(s) and the source, provide a link to the Creative Commons licence, and indicate if you modified the licensed material. You do not have permission under this licence to share adapted material derived from this article or parts of it. The images or other third party material in this article are included in the article's Creative Commons licence, unless indicated otherwise in a credit line to the material. If material is not included in the article's Creative Commons licence and your intended use is not permitted by statutory regulation or exceeds the permitted use, you will need to obtain permission directly from the copyright holder. To view a copy of this licence, visit <http://creativecommons.org/licenses/by-nc-nd/4.0/>.

© The Author(s) 2025